JOURNAL OF CATALYSIS 57, 476–493 (1979)

The Vanadium Pentoxide–Titanium Dioxide System

Structural Investigation and Activity for the Oxidation of Butadiene

GEOFFREY C. BOND AND ANTAL J. SÁRKÁNY[1]

School of Chemistry, Brunel University, Uxbridge, Middlesex UB8 3PH, England

GEOFFREY D. PARFITT

Tioxide International Ltd., Stockton-on Tees, Cleveland TS18 2NQ, England

Received August 8, 1978

The interactions of various anatase and rutile samples with V_2O_5, and their products, have been studied by thermal analysis, by ir and ESR spectroscopy and by X-ray diffraction. The V_2O_5 was introduced either by mechanical admixture or by impregnation of the TiO_2 with NH_4VO_3 and subsequent calcination. With anatase samples containing only low levels of P_2O_5 and K_2O (<0.6%) or containing $SO_4^{=}$ (6.3%), heating to 450 to 600°C leads only to supported V_2O_5: but heating at 750°C produces (i) a change in color to black, (ii) an irreversible loss of oxygen, (iii) a transformation of the anatase into rutile, and (iv) a substantial decrease in surface area. The results of experiments performed with various V_2O_5 concentrations (1 to 60% w/w) suggest that about 8% w/w V_2O_5 becomes incorporated as V^{4+} ions into the rutile lattice during the transformation, through the formation of a compound having the composition $V_{0.04}Ti_{0.96}O_2$. Corresponding processes with rutile take place only at higher temperatures. Anatase containing Na^+ (1.4%) behaves quite differently, and there is evidence for the formation of sodium vanadium bronzes on heating to 450 or 750°C. Catalysts containing supported V_2O_5 oxidize butadiene to maleic anhydride at 260°C with a selectivity which increases with V_2O_5 contents between 1 and 10%, and thereafter remains constant ($S \simeq 0.45$). Those containing the compound $V_{0.04}Ti_{0.96}O_2$ are less active but more selective ($S \simeq 0.57$ for 10 to 30% V_2O_5). With both types, the selective reaction is zero order in butadiene and in O_2, and both show activation energies for selective and for nonselective oxidation of 20 to 25 kcal·mol^{-1}. Selective oxidation is believed to require lattice oxygen, and selectivity correlates with difficulty of reduction by CO.

INTRODUCTION

It is now well established that catalysts containing V_2O_5 are able to catalyze the selective oxidation of butadiene, 1-butene, and benzene to maleic anhydride, and of naphthalene and *o*-xylene to phthalic anhydride. There have been numerous investigations of the effect of promoters and of supports, from which it appears (*1*, *2*) that the combination of V_2O_5 with TiO_2, usually as anatase, exhibits best selectivity and activity, which can be even further enhanced by promoters such as P_2O_5, As_2O_3 (*1*), and K_2SO_4. The physical basis of the success of the V_2O_5–TiO_2 combination is not however clearly established, although there have been several studies of the system's solid state chemistry (*3–5*). It has been observed that, on heating V_2O_5–TiO_2

[1] On leave from Institute of Isotopes, Hungarian Academy of Sciences, P. O. Box 77, Budapest 114, Hungary.

0021-9517/79/060476-18$02.00/0

TABLE 1

Physical Properties and Chemical Compositions of TiO_2 Samples

Sample	Calcination temp/°C	Surface area/ $m^2 g^{-1}$	Crystallite size/Å	Phase	Chemical composition w/w				
					P_2O_5/%	SO_3/%	K_2O	Na^+	CaO
AP1	870	8.9	>1500	Anatase	0.56	0.05	0.36%	33 ppm	97 ppm
AP2	870	8.0	>1500	Anatase	0.56	0.05	0.36%	65 ppm	97 ppm
AP3	702	9.5	>1500	Anatase	0.40	0.05	0.29%	35 ppm	120 ppm
AP4	600	9.6	>1500	Anatase	0.41	0.05	0.29%	37 ppm	<100 ppm
AN	500	98.3	130	Anatase	<0.01	0.1	—	1.4%	—
AS	120	186	130	Anatase	0.35	6.3	0.18%	30 ppm	82 ppm
RP	910	1.5	>1500	Rutile	<0.01	—	18 ppm	0.05%	<20 ppm
RN1	750	11.4	>1500	Rutile	<0.01	0.05	—	5.5%	0.3%
RN2	675	23.9	1000–1500	91% rutile	<0.01	0.07	—	5.3%	0.34%

mixtures, the anatase to rutile phase transformation takes place at a temperature well below that at which it occurs with pure anatase, although the ease of this phase change is notoriously affected by crystallite size and the presence of impurities (*6–8*). There is also a simultaneous loss of oxygen (*5*). It has been suggested (*9*) that "both the reduction of V_2O_5 and the transformation of anatase into rutile are topotactic reactions activated by the remarkable fit of the crystallographic patterns in contact at the V_2O_5–TiO_2 (anatase) interface." In our view, however, this reaction and its product deserve a more precise description.

It is also well established that in working or in used V_2O_5 catalysts the oxidation state of the vanadium falls below five. It has sometimes been thought (*10–12*) that the catalytically active phase is V_6O_{13} (i.e., $V_2O_{4.34}$), although for benzene oxidation the composition $VO_{1.99}$ shows highest selectivity (*13*). For *o*-xylene oxidation over supported V_2O_5 catalysts, however, there is evidence to show that optimum activity and selectivity are found with maximum oxidation state (*1*). In the V_2O_5–TiO_2 system, maximum selectivity in *o*-xylene oxidation is usually observed (*2, 14*) with 10 to 20 mol% V_2O_5 (selectivity ~0.70–0.75), although for 1-butene oxidation the maximum (~0.45) is at 80 mol% V_2O_5 (*15*). Of course it by no means follows that optimum surface requirements are identical for the oxidation of all hydrocarbons.

We have investigated some of the physicochemical properties of the V_2O_5–TiO_2 system using a number of anatase and rutile samples differing in calcination temperature and in the level of impurities, especially Na^+ and $SO_4^=$. We have also assessed the performance of catalysts produced therefrom for the oxidation of butadiene to maleic anhydride, with especial reference to the effect of the temperature to which the catalysts have been heated before use. A clearer picture of the structural chemistry and its connection with catalytic behavior emerges.

EXPERIMENTAL

Materials. The physical properties and chemical compositions of various TiO_2 samples (kindly supplied by Tioxide International Ltd.) are given in Table 1. Other impurities present at levels of 10 to 400 ppm were also detected. The four AP (anatase "pure") samples, which had been calcined at temperatures between 600 and 870°C, had approximately the same levels of impurities (mainly P_2O_5 and K_2O); the AN (anatase–sodium) and RN (rutile–sodium) samples contained mainly Na^+, while the

AS (anatase–sulfate) sample contained about 6% SO_3 (as $SO_4^=$). AP2 was a milled version of AP1.

Before being used in catalyst preparations, the TiO_2 samples were ground and the fraction below 120 mesh was retained. Some catalysts were prepared by "total absorption" impregnation of an aqueous solution of AR grade NH_4VO_3 (ammonium metavanadate), but its solubility in water is low and the maximum attainable V_2O_5 concentrations were about 5% with the AP samples and about 12% for the AN sample. After impregnation, the material was dried at 110°C. To obtain higher V_2O_5 contents, either the TiO_2 sample was added to a solution containing the desired weight of NH_4VO_3 and the excess water was evaporated on a steam bath, with constant stirring, or the NH_4VO_3 was dissolved in oxalic acid solution, in which it is much more soluble, and the "total absorption" procedure followed. Some catalysts were prepared from mechanical mixtures of TiO_2 and V_2O_5, followed by heating to an appropriate temperature. Catalysts containing 1 to 60% V_2O_5 were prepared by one or other of these methods; differences in behavior will be noted where relevant. For structural studies and for investigation of butadiene oxidation, samples were further heated in air either to 450°C for 5 hr to give Y (for yellow) samples or to 750°C overnight to give B (for black) samples. The final figure in the code for the catalyst gives the percentage of V_2O_5: thus AP1B-25 signifies 25% V_2O_5 on anatase AP1 heated to 750°C overnight. All compositions are expressed on a weight basis.

Characterization methods. DTA and TGA measurements were carried out using a Stanton Standata model 6-25 apparatus and a Stanton TRO1 thermobalance, respectively. Gravimetric measurements in N_2 or *in vacuo* were made using a Beckman microbalance Model LM600. ir spectra of samples (650 to 5000 cm^{-1}) were measured with KBr discs using a Unicam SP200 spectrometer. Surface areas were measured by N_2 or Kr adsorption at liquid N_2 temperature in a conventional BET apparatus.

ESR spectra were recorded with a Varian E3 X-band spectrometer with 100-kHz modulation and a modulation width of 1 to 10 G. Samples, contained in a 4-mm tube, were examined either in air at ambient temperature or *in vacuo* at 77 K with 20-mW microwave power. The method of Hecht and Johnston (*16*) was adopted for determining the g factor.

X-Ray diffraction measurements were performed on a Philips unit with Ni-filtered CuK_α radiation using a Debye–Scherrer camera of 11.46-cm diameter. The fraction of rutile in anatase samples X_r was determined by the equation (*17*)

$$X_r = (1 + 0.794 I_a/I_r)^{-1}$$

measuring the intensities of the (110) and (101) reflections for rutile and anatase, respectively. Crystallite sizes were determined by the Scherrer equation (*18*), measuring half-maximum widths. Instrumental broadening was allowed for by Warren's equation (*18*).

Catalytic measurements. Butadiene oxidation was carried out in a conventional flow apparatus at 1 atm pressure; the catalyst was placed in a Pyrex reactor of 1-cm internal diameter and the bed depth was also about 1 cm. Most experiments were performed with a mixture containing about 1.5 mol% butadiene in air, made either by mixing the two gases from cylinders or, when low flow-rates of butadiene were needed, by passing air through two traps in series containing liquid butadiene at −98°C. When investigating the order of reaction with respect to O_2, N_2 was added to keep the butadiene concentration constant. Air and N_2 were passed through a SiO_2 gel tower before use. The outlet tube from the reactor was heated with an ir lamp to prevent condensation of maleic anhydride, which was subsequently collected in a trap cooled in an ice–salt bath for a fixed

time (30 to 120 min). It was then dissolved in H_2O and titrated with standard NaOH solution. Butadiene and CO_2 were analyzed by glc using a 6-m column of 15% w/w dimethylsulfolane on Celite at room temperature; CO was separated from air using a 1-m column of 5A molecular sieve also at room temperature.

The reduction of selected samples by CO was followed with a Beckman microbalance model LM600: The reductant was added after evacuation of the sample to 0.03 Torr at the reaction temperature, and since the extents of reduction were always less than 0.1% there was no noticeable change in pressure.

RESULTS

Characterization by Thermal Analysis

According to preliminary TG studies, NH_4VO_3 impregnated onto anatase decomposed in three steps, at 140°C (weight loss 11.3%), 220°C (−14.9%), and 340°C (−21.4%): The product was V_2O_5. Further work on TGA and DTA was performed only between 400 and 950°C.

On heating AP–V_2O_5 samples in 100 Torr air in the vacuum microbalance, they began to lose oxygen at 660 to 670°C, and temperatures for the maximum rate (T_{max}) were for AP1 and AP2, 720°C, and for AP3 and AP4, 730°C. T_{max} changed only slightly with V_2O_5 concentration. TGA and DTA curves for AP1Y-30 are shown in Figs. 1A–D. The endothermic peak at 690°C is due to the melting of V_2O_5, while that at 740°C corresponds to the process of oxygen loss. When the V_2O_5 content was less than 15% w/w, a second heating did not show either of these peaks; but at higher concentrations a second heating revealed the presence of some remaining V_2O_5 (see Figs. 1C and D). Similar results were obtained with AP2, AP3, and AP4 samples, although AP3 had been prepared at 702°C and AP4 at 600°C (see Table 1).

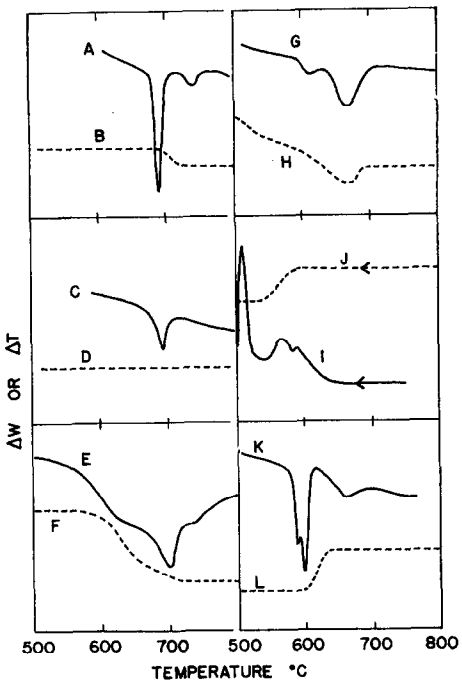

FIG. 1. DTA and TGA results. (A and B) DTA and TGA respectively of sample AP1Y-30, first heating; (C and D) the same, second heating; (E and F) DTA and TGA respectively of sample ASY-30; (G and H) DTA and TGA respectively of sample ANY-30, first heating; (I and J) the same, first cooling; (K and L) the same, second heating.

The gas evolved in the region of 700°C was shown to be oxygen by mass spectrometry.

The extent of oxygen loss measured in air is presented as a function of V_2O_5 content in Fig. 2, together with the results of Cole *et al.* (*5*) for this system. The points fit remarkably well together, except at low V_2O_5 contents.

TGA and DTA of AS–V_2O_5 samples gave similar results, but in this case the presence of SO_3 (6.3% by chemical analysis, 6.7% by TGA) hindered exact determination of oxygen loss. The extents of oxygen loss (Fig. 3) were calculated from the weight losses between 470 and 840°C after correction for the amount of SO_3 lost as estimated from the sample's composition, and assuming that no chemical interaction occurs between SO_3 and V_2O_5. DTA curves were

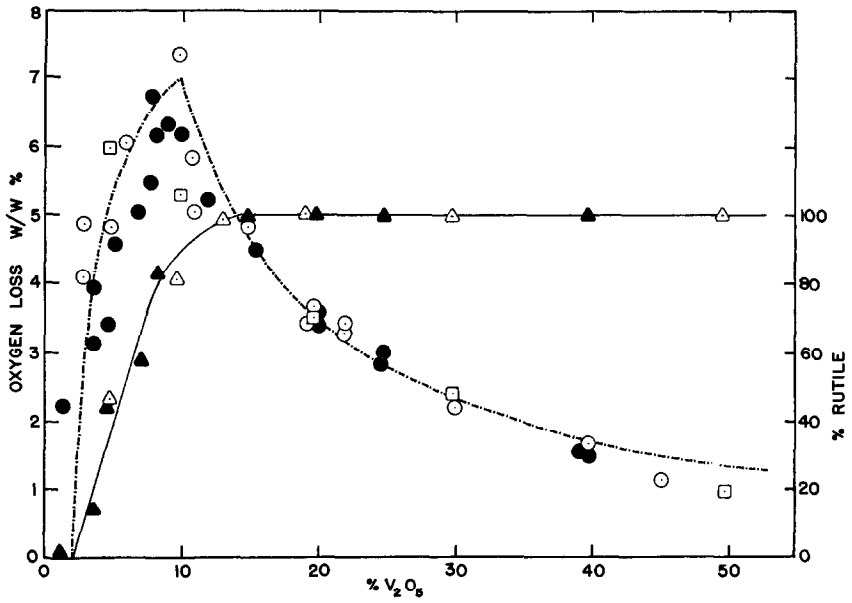

FIG. 2. Extents of oxygen loss (circles) and of anatase transformation into rutile (triangles) as a function of V_2O_5 content. Open points, anatase AP1; filled points, anatase AP2; squares, results of Cole *et al.* (*5*). The curve relating to oxygen loss is calculated as described in the text.

also much affected by the endothermic loss of SO_3 (see Fig. 1 for an example).

Completely different TG and DTA curves were observed using AN anatase as support (Figs. 1G–L). The temperature at which oxygen loss started (T_i) depended on the method used for depositing the V_2O_5 onto the support. For impregnation with NH_4VO_3 dissolved in oxalic acid solution, T_i was 380 to 410°C; for impregnation with aqueous NH_4VO_3 it was 450 to 470°C (Fig. 1H); and for a mechanical mixture of AN anatase and V_2O_5 it was 530 to 540°C. These figures relate to a V_2O_5 content of 30%. With the first two methods, a decrease in the V_2O_5 content was matched by a decrease in T_i. These observations suggest that variation in the particle size of the V_2O_5 may affect T_i. On the first heating, loss of oxygen continued to about 650°C; an increase in weight was then observed, finishing at about 710°C (Fig. 1H). On cooling, oxygen was lost in the region of 650°C in an exothermic process, there being a further sharp exotherm at 510°C not accompanied by a weight change (Figs. 1I and J). On a second heating, oxygen was picked up at about 615°C, apparently in an endothermic step (Fig. 1K and L). To characterize this system we denote the irreversible oxygen loss on first heating as ΔO_i, the reversible change in oxygen content on subsequent heating or cooling as ΔO_r, and the total oxygen deficiency ($\Delta O_i + \Delta O_r$) as ΔO_t. The variation of these quantities with V_2O_5 content is shown in Fig. 4. DTA of the AN sample alone showed a weak exotherm at about 800°C.

To elucidate the effect of TiO_2 structure on the nature of the interaction with V_2O_5, experiments were conducted with the rutile samples RN1 and RN2 which had different anatase contents but about the same sodium content (~5%, see Table 1). According to X-ray analysis, the sodium was mainly in the form of $Na_2Ti_5O_{11}$ ($Na_2O \cdot 5TiO_2$) (*19*). With mechanical mixtures of V_2O_5 and RN samples, oxygen loss began at about 520°C: Oxygen absorption

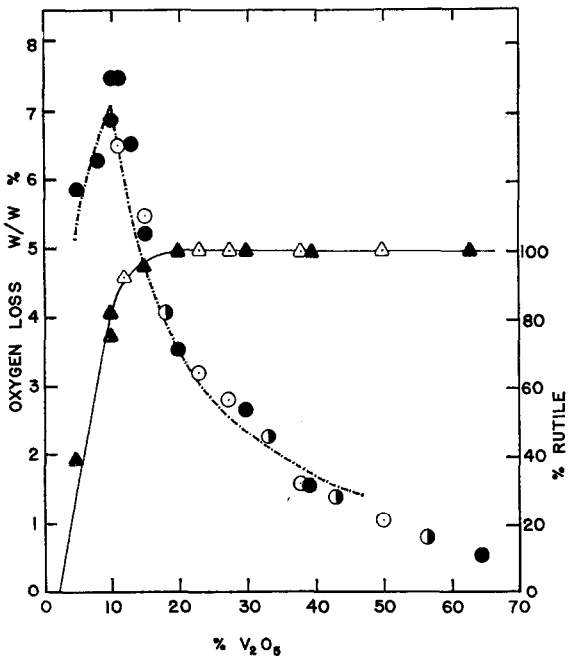

FIG. 3. Extents of oxygen loss (circles) and of anatase transformation into rutile (triangles) as a function of V_2O_5 content. Open points, anatase AP3; filled points, anatase AP4; half-filled points, anatase AS. The curve relating to oxygen loss is calculated as described in the text.

occurred at 680°C, the original weight being almost recovered, and an irreversible oxygen loss was observed at about 820°C. On cooling, oxygen was evolved at 625°C. The maximum amounts of oxygen lost reversibly are shown as a function of V_2O_5 content in Fig. 5: There are clear differences between the extents of oxygen loss

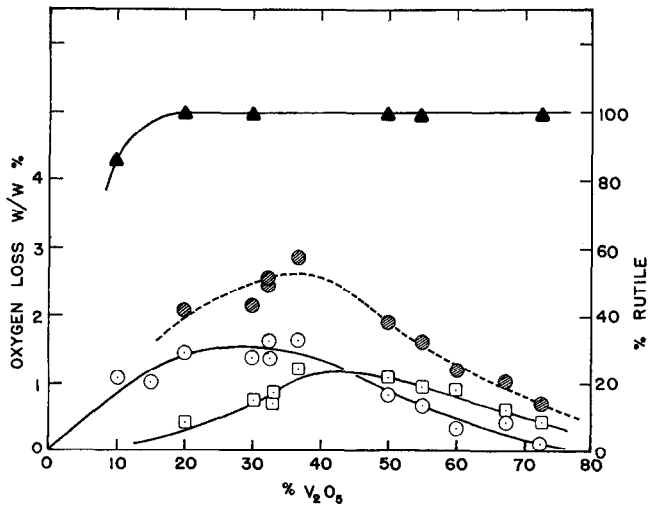

FIG. 4. Extents of irreversible (ΔO_i), reversible (ΔO_r), and total (ΔO_t) oxygen losses, and of anatase transformation into rutile (triangles), for various concentrations of V_2O_5 on anatase AN. ΔO_i, ⊙; ΔO_r, ⊡; ΔO_t, ▨.

with the anatase (AN) and the rutile (RN) samples, but in both cases the low temperature of the initial oxygen loss and the reversibility of oxygen uptake suggest that some kind of chemical reaction takes place between the sodium and the V_2O_5. The point is discussed further below.

With mechanical mixtures of V_2O_5 with "pure" rutile (RP), oxygen loss did not begin below 870°C, and was not readily measurable below about 940°C. Only the endotherm due to the melting of V_2O_5 was observed in DTA. The extent of oxygen loss on heating samples of various V_2O_5 contents to 950°C for 6 hr is shown in Fig. 5: Values are about half those found for the AP samples heated to 750°C.

Structural Characterization by Infrared Spectroscopy

The ir spectrum of V_2O_5 (Fig. 6A) showed a sharp absorption band at 1020 cm^{-1} and a broad one at 840 cm^{-1}: These agree with the literature (*20*), which assigns the former to V=O stretching and the latter to the deformation of V–O–V bridges. Anatase and rutile samples exhibited broad bands in the regions 850 to 650 cm^{-1} and 800 to 650 cm^{-1}, respectively. Further bands at 1600 to 1630 cm^{-1} and at 3300 to 3700 cm^{-1} were due to deformation vibrations of adsorbed water and surface OH groups. The AS sample also showed a broad band at 1100 cm^{-1} with satellites at 1050 and 1130 cm^{-1}, attributable to the $SO_4^{=}$ ion.

The spectra of AP1Y samples (Figs. 6B, D, and F) showed the characteristic band at 1020 cm^{-1}, but the 840 cm^{-1} band was obscured due to the opacity of the support except when the V_2O_5 content exceeded 20%. However, after heating to 750°C (AP1B samples) the former band either disappeared completely (10% V_2O_5) or was barely apparent (15% V_2O_5) or was much reduced in intensity (20% or more V_2O_5) (Figs. 6C, E, and G). Similar results were obtained with the anatase samples AP4 and AS: With the latter it was evident that the 750°C treatment effectively removed the SO_3.

The results obtained with the anatase AN were however quite different. After heating a sample containing 50% V_2O_5 to 450°C, bands were observed at about 1000, 980, and 960 cm^{-1} as well as the 1020 and 840 cm^{-1} bands due to V_2O_5 (Fig. 6H). After heating to 750°C, the bands of V_2O_5 decreased substantially in intensity, while the others increased (Fig. 6I). Similar behavior was seen with 60% V_2O_5; but with 15% and 30% V_2O_5 the bands of V_2O_5 were not seen after heating to either 450 or 750°C and the intensity of the bands between 950 and 1000 cm^{-1} changed relatively little in intensity after heating to the higher temperature (Figs. 6J and K). Re-

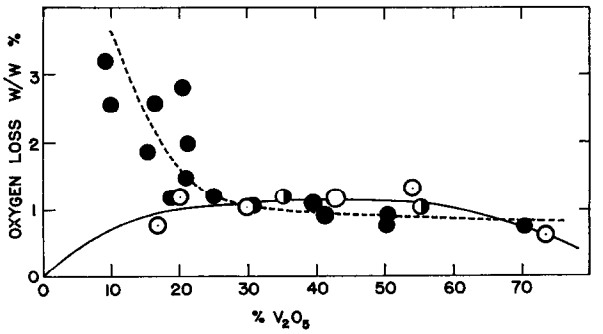

FIG. 5. Extents of oxygen loss from various V_2O_5–rutile samples as a function of V_2O_5 content. ⊙, ◑, Maximum reversible losses with RN1 and RN2 respectively at 600°C; ●, irreversible loss with RP at 950°C.

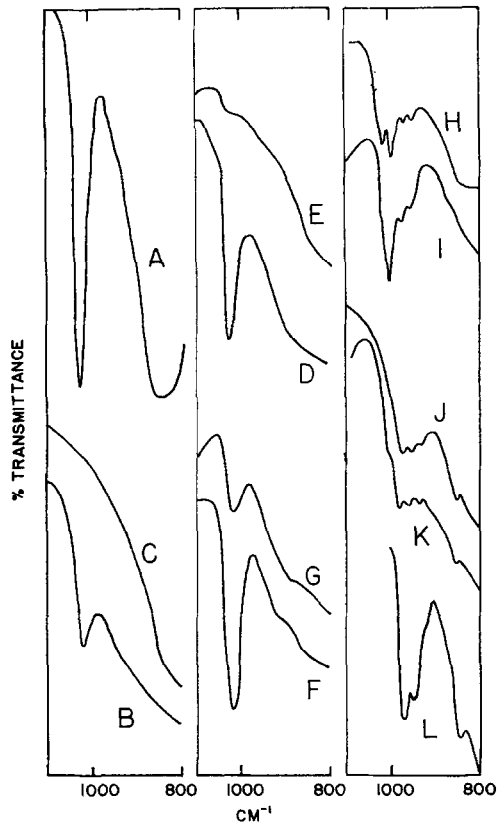

FIG. 6. Infrared spectra of (A) V_2O_5, (B) AP1Y-10, (C) AP1B-10, (D) AP1Y-15, (E) AP1B-15, (F) AP1Y-20, (G) AP1B-20, (H) ANY-50, (I) ANB-50, (J) ANY-15, (K) ANB-15, (L) RN1-17 (800–840°C).

lated bands between 920 and 1000 cm^{-1} were observed when the rutile RN1 containing 17, 31, or 43% V_2O_5 was heated to 800 to 840°C (Fig. 6L). Again it is evident that the sodium impurity in the AN and RN samples causes the reaction with V_2O_5 to follow a quite different course.

The ir spectra of VO_2 and of V_2O_5 showed a continuously increasing absorbance with increasing wave number in the 750 to 1050 cm^{-1} region, with no well-defined bands.

Structural Characterization by X-Ray Diffraction

No trace of rutile was found in either the AP1 or AP2 samples after 5 hr heating at 900°C, but the AN sample showed complete conversion to rutile under these conditions. The weak exotherm seen at 800°C is therefore attributable to this process. This difference is in keeping with the known catalytic effect of cationic impurities on the rate of this phase change.

Diffraction patterns of APY samples indicated that they were a mixture of V_2O_5 and anatase: Typical results are given in Fig. 7. The intensities of the lines did not change after heating in air for 17 hr at either 500 or 600°C. Samples containing less than 3% V_2O_5 showed no distinct lines of V_2O_5.

The patterns shown by the APB samples showed, in agreement with the literature (*3*, *5*), that the polymorphic transformation of anatase into rutile had occurred in

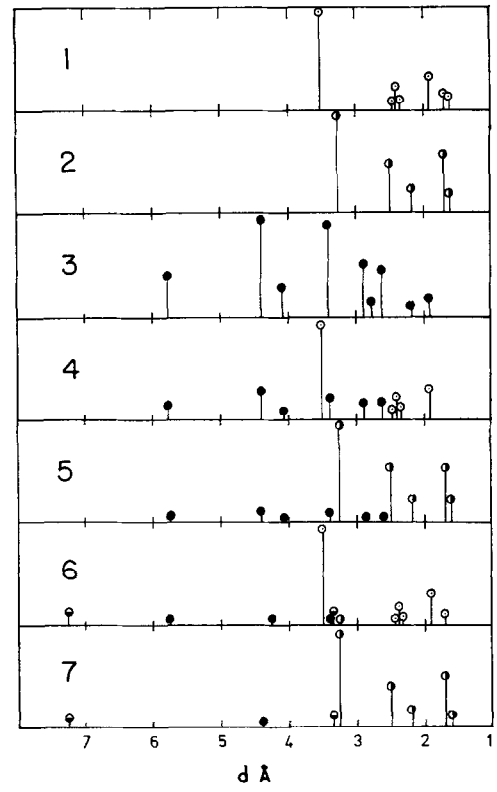

Fig. 7. X-Ray diffraction patterns of (1) anatase, (2) rutile, (3) V_2O_5, (4) AP1Y-30, (5), AP1B-30, (6) ANY-50, (7) ANB-50. Patterns (1) to (3) are taken from Ref. (*13*).

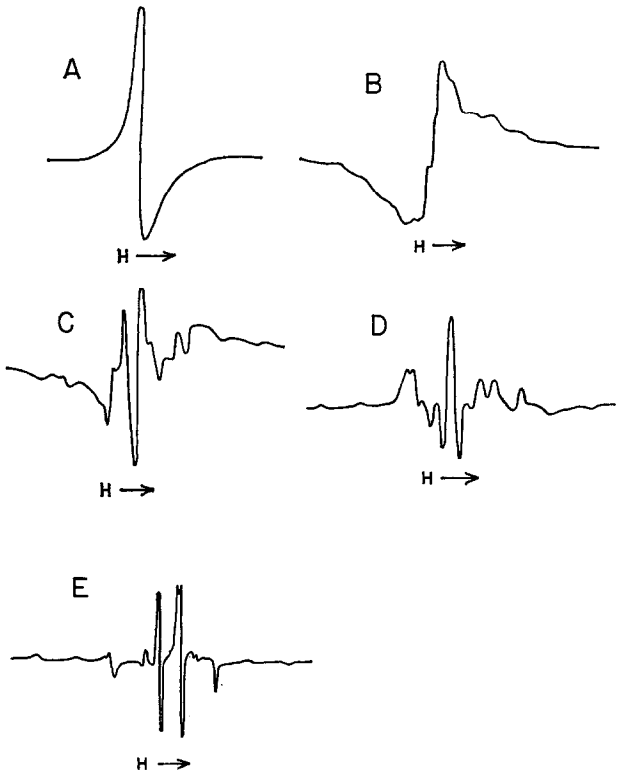

FIG. 8. ESR spectra of (A) AP1Y-20 (air, 24°C); (B) AP1Y-5 (air, 24°C); (C) AP1Y-1 (vacuum, 77°K); (D) AP1B-10 (air, 24°C); and (E) AP1B-10 after heating in air at 750°C for 17 hr (vacuum, 77 K).

parallel with the oxygen loss during heating to 750°C. The extents of transformation as a function of V_2O_5 content are shown in Figs. 2 and 3. X-Ray analysis provided no evidence for the presence of V_2O_5 when its content was below 20%. Above this concentration, however, it was detectable, and its average crystallite size (determined by line broadening) increased rapidly with increasing V_2O_5 content above 20%, being 18 nm at 22%, 34.5 nm at 25%, and greater than 100 nm at 30%.

The lattice parameters for the rutile phase in these samples were determined from the diffraction lines in the back-reflection area by applying Straumanis' method (*18*) to the pairs of $\alpha_1\alpha_2$ doublets. Values of $a = 4.57_8$ Å and $c = 2.95_6$ Å were found for samples containing 15% V_2O_5.

In Fig. 7 (6 and 7) are shown the diffraction patterns of the ANY-50 and ANB-50 samples (heated to 450 and 820°C, respectively). The former shows the lines due to anatase, and the latter those of rutile, but additionally both contain lines which were finally identified as being those of the sodium vanadium bronze $Na_{0.33}V_2O_5$ (*21*). These lines appeared continually in the AN–V_2O_5 system, but were most intense with V_2O_5 contents of 40 to 50%. Their *d*-spacings were difficult to measure precisely because of the degree of line broadening. Samples of ANY containing 15% V_2O_5 exhibited no lines attributable either to V_2O_5 or to a sodium vanadium bronze, presumably because of excessive line broading. However, the ANB-15 sample showed the presence of the bronze $Na_{1.33}V_2O_5$ (*22*) (a weak broad line at

TABLE 2

Parameters of the ESR Spectra

Sample	g	ΔH_{msl}/gauss
AP1Y-50	1.97_3	124
AP1Y-30	1.97_2	143
AP1Y-10	1.97_7	96
AP1Y-1	$g_{\parallel}$ 1.94_3 $g_{\perp}$ 1.98_0	$H_{\parallel}$ 183 $H_{\perp}$ 78
AP1B-30	1.96_8	102
AP1B-10	$g_{\parallel}$ 1.93_2 $g_{\perp}$ 1.98_8	$H_{\parallel}$ 210 $H_{\perp}$ 82
ANY-30	1.97_7	88
ANB-30	1.97_2	92

$d \simeq 5$ Å), as well as of $Na_{0.33}V_2O_5$. The extent of the anatase to rutile transformation on heating to 800°C (Fig. 4) is almost independent of V_2O_5 concentration.

Structural Characterization by ESR Spectroscopy

V_2O_5 obtained by decomposition of NH_4VO_3 in air at 450°C gave an isotropic spectrum of Lorentzian shape for which the g factor was 1.97 and the maximum slope separation ΔH_{msl} was 120 G. This spectrum has often been reported (*23*, *24*) and is assigned to V^{4+} arising from a small oxygen deficiency in the V_2O_5. The APY samples containing 5 to 50% V_2O_5 had a similar g value but variable line widths (see Figs. 8A and B for examples). The parameters are collected in Table 2. AP1Y samples with low V_2O_5 contents always showed a poorly resolved hyperfine structure (Fig. 8C) due to dipole–dipole interactions (*25*). This spectrum can be assigned to VO^{2+} ions having a square pyramidal coordination (*26*). AP1B samples having 5 to 10% V_2O_5 exhibited similar spectra (see for example Fig. 8D), the g factors being collected in Table 2. With V_2O_5 contents greater than 10%, only a slightly asymmetric singlet spectrum was found. Heating the AP1B-5 and −10 samples in air overnight at 750°C decreased the intensity of the signals and they were completely destroyed by heating overnight in nitrogen at this temperature. Due to the short relaxation time, samples heated in air exhibited ESR spectra at 77 K (Fig. 8E): The separation of the horizontal component is about 185 G, while that for the perpendicular one is nearly 70 G. This spectrum has been assigned to VO^{2+} on the basis of measurements made with polycrystalline rutile samples doped with V^{4+} (*4*, *27*).

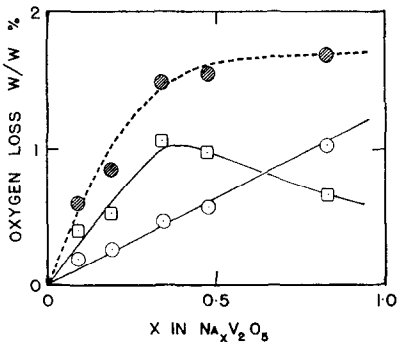

FIG. 9. Extents of irreversible (ΔO_i), reversible (ΔO_r), and total (ΔO_t) oxygen losses as a function of the Na/V_2O_5 molar ratio in mixtures of Na_3VO_4 and V_2O_5. ΔO_i, ⊙; ΔO_r, ⊡; ΔO_t, ▨.

ANY and ANB samples containing 15 to 60% V_2O_5 showed only a sharp signal of Lorentzian shape. The values of g and of ΔH_{msl} did not change much with composition; typically g was 1.97 and ΔH_{msl} 87 G. The value of ΔH_{msl} is smaller than the value of 210 G reported (*28*) for $Na_zV_2O_5$. The very sharp ESR spectra are probably due to exchange narrowing (*25*), suggesting that the V^{4+} centers are very close together on the surface.

TABLE 3

Surface Area Measurements

Percentage V_2O_5[a]	Surface area/m^2 g^{-1}	
	Y samples	B samples
5	8.6	2.2
10	8.4	1.3
15	8.4	1.1
20	8.5	0.8

[a] Supported on anatase AP1.

Surface Area Measurements

Surface areas of AP1Y samples were only slightly lower than that of the support itself (see Table 1) and were independent of V_2O_5 content. However, heating to 750°C to produce the AP1B samples led to a more than fourfold decrease in area (see Table 3).

Catalytic Behavior of V_2O_5–Anatase Samples Heated to 450°C

Initial experiments on butadiene oxidation with sample AP1Y-15 at 248°C showed that its activity decreased rapidly during the first 2 hr of use, during which time it changed color from yellow to dark brown and the reaction became more selective: Thereafter the activity and selectivity remained constant for 15–20 hr (Fig. 10). Similar behavior was seen with other V_2O_5 contents. Activity increased after overnight treatment in O_2 at 400°C, but soon returned to its original values. Kinetic studies were performed after the activity had stabilized. At short contact times, butadiene removal showed first-order behavior and the selectivity (defined as maleic anhydride formed/butadiene removed) was constant; but at longer contact times the selectivity decreased progressively as the contact time was increased. The selectivities quoted below are those obtained at short contact times. CO_2 yields were about five times larger than those of CO.

In Fig. 11 rates of butadiene removal and selectivities measured at 260°C are plotted against the V_2O_5 contents of catalysts containing up to 30% V_2O_5 on anatase AP1: Activities are expressed per gram catalyst, since surface areas decrease only slightly with increasing V_2O_5 content (Table 3). Both activities and selectivities initially increase rapidly as the V_2O_5 content is increased, but there is no further effect on either above 10% V_2O_5.

Apparent activation energies for butadiene removal (E_{BD}) were measured between about 220 and 300°C. Orders of reaction were measured with catalysts containing 5 and 15% V_2O_5 at 240°C and also with the anatase AP1 alone at 390°C: with the former, separate values were derived from the effects of partial pressure variation on butadiene removal (m_{BD}, n_{BD}) and maleic anhydride formation (m_{MA}, n_{MA}) (see Table 4). No formation of maleic anhydride was observed with the anatase. The n_{MA} orders in O_2 were about zero, but the n_{BD} orders were about 0.3: Increasing the O_2 content of the reactant gas stream thus depresses the selectivity, but this is due entirely to the increased rate of CO and CO_2 formation.

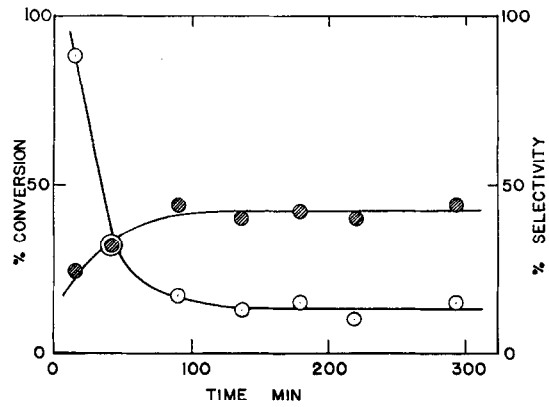

FIG. 10. Dependence of conversion of butadiene (open points) and selectivity (hatched points) on time for sample AP1Y-15 (248°C: 1 5 mol% C_4H_6; 0.46 $cm^3\ s^{-1}$).

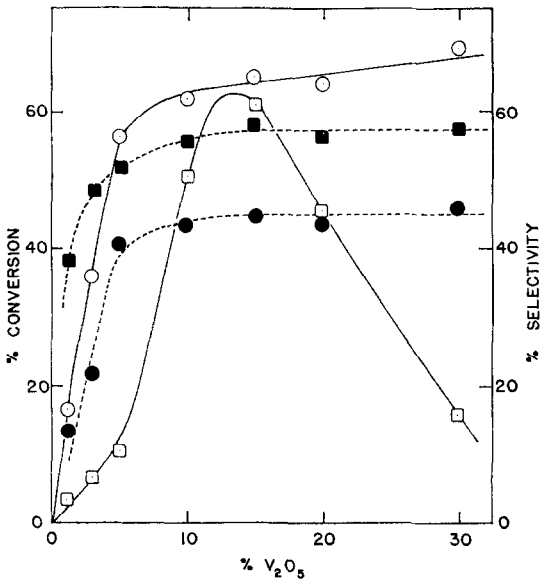

FIG. 11. Dependence of conversion of butadiene (open points), and of selectivity (filled points), upon V_2O_5 content for AP1Y (circles) and AP1B samples (squares).

Neither ir spectroscopy nor X-ray diffraction gave any indication that catalysts after use contained any vanadium compound other than V_2O_5. Although the change in color signifies reduction, it was probably confined to a very thin layer at the surface.

Catalytic Behavior of V_2O_5–Anatase Samples Heated to 750°C

The B samples showed no initial loss of activity or increase in selectivity and were stable over the 15- to 20-hr periods in which they were studied. The variation in the rate of butadiene removal and of selectivity with V_2O_5 content at 300°C are also shown in Fig. 11. The activity at first rises more slowly than was the case with the Y samples, although the selectivity increases more rapidly. There is a quite sharp maximum in activity at 15% V_2O_5, whereafter it falls rapidly although the selectivity does not fall. Consistently higher selectivities are shown by the B samples.

TABLE 4

Kinetics of Butadiene Oxidation[a]

Catalyst	m_{BD}	n_{BD}	m_{MA}	n_{MA}	E_{BD}/kcal mol^{-1}	E_{MA}/kcal mol^{-1}	S_{max}[b]
AP1	0.36	0.93	—	—	27	—	0
AP1Y-5	0	0.27	0.07	−0.07	21	20	0.43
AP1Y-10	—	—	—	—	23	23	0.45
AP1Y-15	−0.07	0.29	0.03	0	24	24	0.43
AP1B-5	0.05	0.43	0.03	−0.12	22	22	0.48
AP1B-10	—	—	—	—	25	24	0.58
AP1B-15	−0.11	0.23	−0.05	−0.15	25	24	0.58

[a] The subscript BD refers to the process of butadiene removal; MA refers to maleic anhydride formation. Rates are proportional to $P_{C_4H_6}{}^m P_{O_2}{}^n$.

[b] The maximum selectivity observed in the temperature range used for measuring the activation energies.

Apparent activation energies were determined between 280 and 360°C for catalysts having 5, 10, and 15% V_2O_5 (see Table 4). Orders of reaction were obtained by the two methods at 300°C with catalysts having 5 and 15% V_2O_5: They are generally similar to those found with the Y samples.

Reduction of V_2O_5–TiO_2 Catalysts by CO

Studies of the isothermal reduction of catalysts by CO were undertaken to obtain more information on the reactivity of lattice oxygen in the valious samples used for the catalytic work. Rates of reduction of AP1 and of RP alone were very low between 350 and 500°C, but at this temperature the final weight losses under 100 Torr CO corresponded to about 0.025 and 0.01 mg O_2 per 100 mg sample, respectively. Assuming that the (011) and (110) planes in anatase and rutile are preferentially exposed (*29*), these weight losses correspond respectively to the removal of about 5 and 12% of the surface oxygen.

Rates of reduction of Y and B samples of V_2O_5–TiO_2 by CO were however readily measurable between 390 and 480°C. Losses in weight at first increased linearly with time, but subsequently the parabolic rate law was accurately followed (Fig. 12). Rates from the linear portion were measured at 450°C and 100 Torr CO, and these together with the activation energies are plotted as a function of V_2O_5 content in Fig. 13. The activation energies for the Y samples do not change significantly with increasing V_2O_5 content, but the rates increase steadily and significantly. With the B samples, however, activation energies are somewhat higher, are maximal at 15% V_2O_5, and then decrease until at 30% V_2O_5 the values for the Y and B samples are not much different. Reduction rates for the B samples are some two orders of magnitude lower than for the Y samples but also tend to increase with increasing V_2O_5 content. Rates were proportional to initial CO pressure.

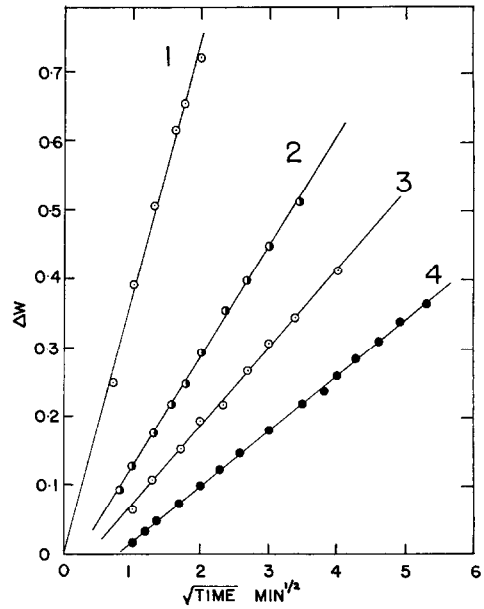

FIG. 12. Parabolic rate law plots for reduction by CO and C_4H_6. (1) AP1Y-15 at 360°C, 100 Torr C_4H_6; (2) AP1B-15 at 340°C, 100 Torr C_4H_6; (3) AP1Y-15 at 430°C, 100 Torr CO; (4) AP1B-15 at 480°C, 100 Torr CO.

Reduction by butadiene was briefly examined with samples AP1Y-15 and AP1B-15: Rates were much faster than with CO (see Fig. 12) but also followed the parabolic rate law. They were independent of initial butadiene pressure in the range 2 to 200 Torr.

DISCUSSION

Reaction of V_2O_5 with "Pure" Anatase below 600°C

All the experimental evidence points to the absence of any interaction between V_2O_5 and the AP samples on heating in air at temperatures up to 600°C. The ESR spectra of samples containing 10 to 50% V_2O_5 are similar and agree with that of V_2O_5 alone. The Lorentzian shape of the spectra suggests an electronic exchange interaction between V^{4+} ions (*25*), signifying that they are clustered (*24*). The ESR results are therefore also consistent with

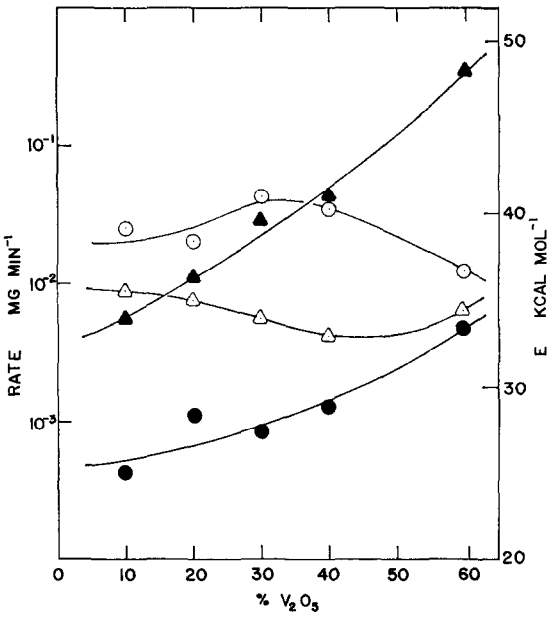

FIG. 13. Dependence of rates of reduction by CO (mg g^{-1} min^{-1}) (filled points) and of activation energies (open points) for this process upon V_2O_5 content for AP1Y (triangles) and AP1B samples (circles). Rates measured at 450° and 100 Torr CO.

the existence of V_2O_5 as a separate phase. The formation of square-pyramidally coordinated VO^{2+} ions only occurs at low V_2O_5 concentrations.

Reaction of V_2O_5 with "Pure" Anatase and "Pure" Rutile above 700°C

On heating any of the AP anatase samples with V_2O_5 added by any of the three methods used to about 700°C (i.e., just above the melting point of V_2O_5, which is 690°C), oxygen is evolved (Fig. 2), and our results strongly suggest, in confirmation of those of other workers (*3–5*), that this is due to the partial or complete reduction of V^{5+} to V^{4+}. No evidence has been found for any lower oxidation state of vanadium, or for nonstoichiometric lower oxides of titanium. The extent of oxygen loss with the sulfate-containing AS sample (Fig. 3) was similar, after allowing for the loss of SO_3. The maximum loss of oxygen occurs at about 10% V_2O_5, corresponding to a mole fraction of about 0.05. The extent of the maximum oxygen loss is not well defined, but lies between 0.35 and 0.40 mol O_2 per mol V_2O_5: The declining extent of oxygen loss to the right of the maximum clearly shows that at higher concentrations of V_2O_5 the reduction is only partial.

We interpret the results as follows. We suppose that the first 2% of V_2O_5 is inactivated by the impurities present (perhaps due to the formation of a potassium vanadium bronze), and that V_2O_5 in excess of 2% only is capable of reduction to VO_2. We further suppose that at most a further 8% V_2O_5 can be reduced. Calculated curves based on these suppositions are shown in Figs. 2 and 3, and describe the results well except perhaps at high V_2O_5 concentrations. The quantity of V_2O_5 capable of being reduced is thus about 8% by weight (mole fraction ~0.04).

Simultaneously with this reduction there occurs the polymorphic transformation of anatase into rutile (*3, 5*): This is an order–disorder transition involving changes in secondary coordination (*6, 7*). In both

structures the Ti^{4+} ions are octahedrally coordinated to oxide ions, but anatase has three short oxide–oxide distances while rutile has only two. Conversion to rutile is clearly catalyzed by the presence of V_2O_5, and it is interesting that Pt, PdO, and RuO_2 are also catalysts (*30*), although only RuO_2 has the rutile structure. The change to rutile is complete at a V_2O_5 concentration only a little higher than those at which the oxygen loss is a maximum (see Figs. 2 and 3): Below this, the extent of the transformation is proportional to the effective V_2O_5 concentration. This excludes the possibility that the rutile formed acts as a seed for the transformation. The completeness of the structural change is underlined by the very substantial decrease in surface area which accompanies it (Table 3).

With samples containing 1 to 15% V_2O_5 heated to 750°C, neither thermal analysis nor ir spectroscopy nor X-ray diffraction provides evidence for the separate existence of V_2O_5 or of VO_2. We therefore conclude that the V^{4+} ions are present in solid solution in the rutile lattice; that the maximum mol fraction of V^{4+} able to be dissolved is about 0.04; and that the V^{4+} ions enter the TiO_2 lattice during the phase transformation. V_2O_5 in excess of this concentration remains as such and is observable. The incomplete transformation in the 1 to 10% V_2O_5 range suggests the formation of a compound $V_{0.04}Ti_{0.96}O_2$. To summarize, when V_2O_5 concentration is between 1 and 10% the main components are unchanged anatase and the solid solution: At higher concentrations they are the solid solution and V_2O_5.

The formation of such a pseudobinary solid solution is well known from direct melting studies (*31*). VO_2, which has the MoO_2 structure at low temperature, transforms at about 70°C to a rutile structure, and the solid solution has been prepared by flame fusion and arc melting methods.

The mechanism by which V^{4+} ions enter the TiO_2 lattice at about 700°C is uncertain. Neither the temperature of precalcination nor the surface area affects the temperature at which the process occurs (compare the behavior of the AP and AS samples). Loss of oxygen on heating V_2O_5 with "pure" rutile (RP sample) is only readily measurable at about 950°C, showing that incorporation of V^{4+} ions into the rutile lattice is much more difficult than into the lattice undergoing the phase change. The extent of oxygen loss after 6 hr at 950°C (Fig. 5) is almost exactly half that shown with the AP samples at 750°C, but the form of its dependence on V_2O_5 content strongly suggests that again only a limited quantity of V^{4+} ions can be incorporated. The calculated curve shown in Fig. 5 is based on the assumption that 4% of the V_2O_5 only is incorporated under the conditions of these experiments.

We believe the incorporated V^{4+} ions occupy substitutional rather than interstitial positions in the rutile lattice: This has a tetragonal structure, with TiO_6 octahedra joined by edges and corners, each oxide ion being shared by three octahedra (*32*). In consequence of this type of coupling, there are open channels with octahedral interstitial positions. ESR studies (*33*) on doped single rutile crystals indicate that Ti^{3+} ions can occupy these sites, whereas V^{4+} ions can occupy only substitutional positions. The ESR spectrum of sample AP1B-10 measured at 77 K agrees with that of V^{4+} reported in that paper.

Additional evidence for substitutional incorporation comes from the values of the lattice parameters of the rutile phase. These (a = 4.57 Å and c = 2.95 Å) are *smaller* than those observed (*32*) for pure rutile (a = 4.593 Å and c = 2.959 Å), showing that contraction has occurred, especially in the x and y directions. This is understandable only if the smaller V^{4+} ion has replaced some of the Ti^{4+} ions in the lattice (V^{4+}, 0.58 Å; Ti^{4+}, 0.61 Å). This result cannot be due to an oxygen-deficient rutile phase (*32*), since $TiO_{1.9}$ has an *expanded*

rutile lattice (a = 4.603 Å and c = 2.960 Å).

Reaction of V_2O_5 with Anatase Containing Sodium

The manner in which V_2O_5 reacts with sodium-containing anatase (AN) and rutile (RN) samples is quite different from that previously described for the relatively pure materials. In the case of the AN material, we believe that the V_2O_5 reacts with sodium to form one or more sodium vanadium bronzes (*20*): These are responsible for the ir bands observed between 950 and 1000 cm^{-1}. The bronze of composition $Na_{0.33}V_2O_5$, which has been identified through its *d*-spacings, may be formulated as $Na_2O \cdot 2VO_2 \cdot 5V_2O_5$: Bronze formation therefore requires partial reduction of the V_2O_5, and the oxygen evolved in this reduction is that irreversibly lost on heating (Fig. 1H) and denoted as ΔO_i, or perhaps this plus the reversible loss ΔO_r. Isothermal treatments followed by ir spectroscopy show that the bronze is formed to a substantial extent at 450°C, but that more is formed on heating to 750°C. The weak endotherm at 600°C observed in the first heating (Fig. 1G) we associate with the melting of the bronze, for it appears as a sharp and stronger endotherm in the second heating, when there is no weight change, and also as a sharp exotherm at 510°C on cooling: The bronze is also capable of taking up and evolving oxygen reversibly in the 500 to 700°C range.

As we could find no mention in the literature of such a reversible oxygen uptake, additional TGA experiments were undertaken with Na_3VO_4 and V_2O_5 mixtures. They showed characteristics similar to those in Figs. 1G and H, and the oxygen losses ΔO_r, ΔO_i, and ΔO_7 as a function of x in $Na_xV_2O_5$ are shown in Fig. 9. However, the expected loss of $\frac{1}{12}$ or 0.083 mol O_2 per mol V_2O_5 when x is 0.33 agrees only with ΔO_t and not with ΔO_i. ΔO_i not unnaturally increases with x, but ΔO_r passes through a maximum at $x \simeq 0.4$. Turning now to the interpretation of Fig. 4 and considering first the right hand side: The progressive addition of *sodium-containing anatase to V_2O_5* equates to the progressive increase in x in Fig. 9. The relative sizes of ΔO_i, ΔO_r, and ΔO_t are about the same between 70 and 50% V_2O_5 in Fig. 4 as between x values of 0.1 to 0.6. Concerning the low V_2O_5 content side of Fig. 4 we are less certain. Presumably the V_2O_5 initially reacts with part but not all of the sodium, perhaps forming bronzes with x greater than unity: These are apparently characterized by values of ΔO_i greater than ΔO_r, unlike the bronzes of low sodium content, but the ratio of mol O_2 lost/mol V_2O_5 never rises to the value of 0.33 expected for $Na_{1.33}V_2O_5$. Further work would be required to achieve a full interpretation of Fig. 4.

At 820°C the anatase to rutile transformation also occurs, and is complete above 20% V_2O_5. We cannot be sure whether this is accompanied by V^{4+} ion incorporation as with the AP anatases, but since we have shown that the change occurs in the absence of V_2O_5 at 900°C it must be considered unlikely, and the measurements of oxygen loss offer no support.

Oxidation of Butadiene

We consider first the results obtained with low Na^+ anatase samples containing various amounts of V_2O_5 and heated to 600°C (Y samples). The rates of butadiene removal increase markedly with V_2O_5 content up to 5% (Fig. 11), due presumably to an increase in the area of V_2O_5 available to the reactants, but thereafter there is little further increase, presumably because surface areas do not vary much with V_2O_5 contents above 5% (Table 3). Activation energies and orders of reaction show little difference between AP1Y-5 and AP1Y-15 samples (Table 4); the low selectivities observed with 1 and 3% V_2O_5 are probably

due to inactivation of the V_2O_5 by impurities present in the anatase, as noted above. Rates of reduction by CO at 450°C however continue to rise in the range of 5 to 30% V_2O_5, without there being a significant change in activation energy (Fig. 13): The effect must therefore be due to an increase in the fraction of surface active *in this reaction.* Increase in O_2 pressure is without effect on the rate of maleic anhydride formation, although it affects the production of CO and CO_2 considerably (Table 4): This clearly indicates that, in common with other selective oxidations, the partially oxidized product is formed by the use of lattice oxygen while the nonselective reaction involves adsorbed oxygen species (*34, 35*). In the case of V_2O_5-containing catalysts, the lattice oxygen species in question may be the extralamellar atoms which are doubly bonded to V^{5+} ions (*36*).

The phase transformation which occurs on heating "pure" anatase with V_2O_5 to 750°C is also accompanied by a four- to eightfold decrease in surface area (Table 3); this goes some way to explain the lower activity of the B samples in butadiene oxidation (Fig. 11), and also in removal of lattice oxygen by CO (Fig. 13). However, while the activation energies E_{BD} and E_{MA} (Table 4) for the Y and B samples of the same V_2O_5 content are not much different, activation energies for reduction by CO are significantly higher for the B samples than for the Y samples (Fig. 13). It is of interest that the values approach each other when the V_2O_5 content reaches 30%, since at this point the B samples contain some 20% free V_2O_5.

The dependence of the rate of butadiene removal on V_2O_5 content follows a quite different form with the B samples (Fig. 11): The activity initially rises more slowly than with the Y samples, passes through a maximum at 15% V_2O_5, and then declines rapidly. Selectivities are higher throughout. The activity curve to the left to the maximum mirrors closely that for the extent of formation of the rutile-like $V_{0.04}Ti_{0.96}O_2$ phase, and we are therefore inclined to say that the more highly selective but slower reaction occurs on this phase. This conclusion is supported by the fact that this phase contains V^{4+} ions, and by the observation that catalysts containing it do not exhibit any induction period. The decrease in activity to the right of the maximum may be assigned to the progressive obfuscation of the binary oxide phase by V_2O_5: But we cannot explain why the free V_2O_5 which so clearly exists in this region is not itself catalytically active.

The kinetic results (Table 4) may be generalized in the statement covering both types of catalyst that the selective reaction is about zero order in both reactants, while the nonselective reaction is of zero order in butadiene but of a fractional positive order in O_2. Thus there can be no fundamental difference in the mechanisms of the reactions over the Y and B samples. The higher selectivity exhibited by the latter however correlates clearly with their greater difficulty of reduction by CO. This constitutes a further instance of a greater difficulty of removing lattice oxygen correlating with higher selectivity (*15, 37*). If indeed as we believe the active phase in the more selective reaction is the binary oxide $V_{0.04}Ti_{0.96}O_2$, it may be that only those oxide ions adjacent to V^{4+} ions are reactive both in butadiene oxidation and in reduction by CO. This would provide an additional reason for the lower activity of the B samples.

ACKNOWLEDGMENT

A.J.S. is indebted to Tioxide International Ltd for the award of a Fellowship during the tenure of which this work was carried out.

REFERENCES

1. Wainwright, M. S., and Hoffman, T. W., *Canad. J. Chem. Eng.* **55**, 552, 557 (1977).
2. Vanhove, D., and Blanchard, M., *J. Catal.* **36**, 6 (1976); *Bull. Soc. Chim. France* 3291 (1971).

3. Yoshida, S., Murakami, T., and Tarama, K., *Bull. Inst. Chem. Res. Kyoto Univ.* **51**, 195 (1973).
4. Piechotta, M., Ebert, I., and Scheve, J., *Z. Anorg. Allg. Chem.* **368**, 10 (1969).
5. Cole, D. J., Cullis, C. F., and Hucknall, D. J., *J. Chem. Soc. Farad. Trans. I* **72**, 2185 (1976).
6. Sullivan, W. F., and Coles, S., *J. Amer. Ceram. Soc.* **42**, 127 (1959).
7. Yoganarasimhan, S. R., and Rao, C. N. R., *Trans. Faraday Soc.* **58**, 1579 (1962).
8. Rao, C. N. R., Turner, A., and Honig, J. M., *J. Phys. Chem. Solids* **11**, 173 (1959).
9. Vejux, A., and Courtine, P., *J. Solid State Chem.* **23**, 93 (1978).
10. Simard, G. L., Steger, J. F., Arnott, R. J., and Siegel, L. A., *Ind. Eng. Chem.* **47**, 1424 (1955).
11. Vol'fson, V. Ya., and Gauyuk, N. L., *Kinet. Katal.* **6**, 306 (1965).
12. Colpaert, M. N., *Z. Phys. Chem. (Frankfurt)* **84**, 150 (1973).
13. Schaefer, H., *Ber. Bunsenges. Phys. Chem.* **71**, 222 (1967).
14. Grabowski, R., Grzybowska, B., Haber, J., and Sloczynski, J., *Reaction Kinet. Catal. Lett.* **2**, 81 (1975).
15. Blanchard, M., Louguet, G., Rivasseau, J., and Delgrange, J.-C., *Bull. Soc. Chim. France* 3071 (1972).
16. Hecht, H. G., and Johnston, T. S., *J. Chem. Phys.* **46**, 23 (1967).
17. Spurr, R. A., and Myers, H., *Anal. Chem.* **29**, 760 (1957).
18. Klug, H. P., and Alexander, L. E., "X-Ray Diffraction Procedures." Wiley, New York, 1970.
19. ASTM X-Ray Powder Data File, 1973, No. 11-289.
20. Frederickson, L. D., and Hanson, D. M., *Anal. Chem.* **35**, 818 (1963); Kera, Y., and Mirota, K., *J. Phys. Chem.* **73**, 3973 (1969); Nyquist, R. A., and Kagel, R. O., "Infrared Spectra of Inorganic Compounds (3800–45 cm^{-1})," pp. 215–217. Academic Press, London/New York, 1971.
21. Pollman, Z. P., *Z. Anorg. Allg. Chem.* **340**, 208 (1965); Bevan, D. J. M., and Hagenmuller, P., "Non-Stoichiometric Compounds: Tungsten Bronzes, Vanadium Bronzes and Related Compounds." Pergamon, Oxford, 1973; Pletneva, E. D., Khodos, M. Y., Fotiev, A. A., and Volkov, V. L., *Russ. J. Phys. Chem.* **51**, 885 (1977).
22. Pouchard, M., *Bull. Soc. Chim. France* 4343 (1967).
23. Mann, R. S., and Khulbe, K. C., *Bull. Chem. Soc. Japan* **45**, 2929 (1972); Mirota, K., and Kuwata, K., *Bull. Chem. Soc. Japan* **36**, 229 (1963).
24. Takahashi, H., Shiotani, M., Kobayashi, H., and Sohma, J., *J. Catal.* **14**, 134 (1969).
25. Anderson, P. W., and Weiss, T. R., *Rev. Mod. Phys.* **25**, 1269 (1953).
26. Van Reijen, L. L., and Cossee, P., *Disc. Faraday Soc.* **41**, 277 (1966).
27. Gesmundo, F., Rossi, P. F., Asmundis, C., Torlaschi, S., and Aspes, P., *Ann. Chim.* 218 (1971); Siegel, I., *Phys. Rev.* **134A**, 193 (1964).
28. Gendel, I., Cotts, R. M., and Sienko, M. J., *J. Chem. Phys.* **37**, 220 (1962).
29. Winchell, A. N., and Winchell, H., "Elements of Optical Mineralogy," Part II, pp. 66 ff. Wiley, New York, 1955.
30. Brystrov, V. I., Avksentev, V. V., and Sokolov, V. A., *Russ. J. Phys. Chem.* **10**, 1441 (1973).
31. Marinder, B. O., and Magneli, A., *Acta. Chem. Scand.* **11**, 1635 (1957); Sakata, K., and Sakata, T., *J. Appl. Phys. Japan* **6**, 112 (1967).
32. Andersson, S., Collen, B., Kuylenstierna, U., and Magneli, A., *Acta Chem. Scand.* **11**, 1641 (1957); Andersson, S., *Acta Chem. Scand.* **11**, 1653 (1957).
33. Yamaka, E., and Barnes, R. G., *Phys. Rev.* **135A**, 144 (1964); Gerritsen, H. J., and Lewis, H. R., *Phys. Rev.* **119**, 1010 (1960).
34. Butt, N. S., Fish, A., and Saleeb, F. Z., *J. Catal.* **5**, 508 (1966).
35. Juusola, J. A., Mann, R. F., and Downie, J., *J. Catal.* **17**, 106 (1970).
36. Tarama, K., Teranishi, S., Yoshida, S., and Tamura, N., *in* "Proc. 3rd Internat. Congr. Catalysis," Vol. 1, p. 282. North Holland, Amsterdam, 1965.
37. Sachtler, W. M. H., Dorgelo, G. J. H., Fahrenfort, J., and Voorhoeve, R. J. H., *in* "Proc. 4th Internat. Congr. Catalysis," Vol. 1, p. 454. Akadémiai Kiadó, Budapest, 1971.